International Journal of Modern Engineering Research (IJMER)

www.ijmer.com Vol.2, Issue.1, pp-009-015 ISSN: 2249-6645

Anisotropic Dry Etching (RIE) for Micro and Nanogap Fabrication

Th. S. Dhahi[1], U. Hashim[2]

[1,2] Institute of Nano Electronic Engineering, University Malaysia Perlis (UniMAP)

ABSTRACT

The main objective of this research is to develop a micro and nanogap structure using dry anisotropic etching –Reactive Ion Etching- RIE. Amorphous silicon material is used in the micro and nanogap structure and gold as electrode. The fabrication processes of the micro and nanostructure are based on conventional photolithography, wet etching for the Al pattern and wet etching for a-Si pattern using RIE process. Reactive ion etching (IP-RIE) has been applied and developed as essential method for etching micro and nanogap semiconductors. The fabrication and preparation methods to fabricate micro and nanogaps using RIE properties are discussed along with their advantages towards the nanotechnology and biodetection. In this research, 2 masks designs are proposed. First mask is the lateral micro and nanogap and the second mask is for gold pad electrode pattern. Lateral micro and nanogaps are introduced in the fabrication process using amorphous silicon and gold as an electrode. As a result we need to deposit Al layer over the amorphous silicon semiconductor material before coating a photoresist to protect the a-Si layer during the etching and using the Al layer as a hard mask. The requirement time to etch 1µm amorphous silicon pattern completely by using IP-RIE to fabricate the micro and nanogap structure its take approximately 30sec. These results are better than those using wet anisotropic etching techniques.

Keywords - **Micro and nanogap, photolithography, reactive ion etching (RIE).**

1. INTRODUCTION

The RIE equipment used in these experiments was a Vacutech parallel-plate system. The lower electrode is powered by a 13.56 MHz-RF generator coupled through an automatic tuning network. Each electrode is 200 mm in diameter and the distance between them is 23 mm. The RF electrodes are made of anodised aluminium. The chamber volume is 131 and the system is pumped by a 350 l/rain lurbomolecular pump backed by a mechanical rotary vane pump. The base pressure before each run was less than 5 x 10 Tort. A two-level factorial design of experiments was used to find the main and interaction effects governing etch rate and sidewall slope. Even through the RIE process performance is influenced by interaction effects between different factors, such as, oxygen content, power density, pressure and loading, at a chosen set of etching parameters.

Different techniques and schemes such as, sandblasting, mechanical grooving, and wet chemical etch; laser

sculpturing and plasma etching have been used to texture the surface of single and polycrystalline silicon. One of the characteristics of all these methods is that they use either chemical- or physical-etching mechanisms to produce the desired pattern. This imposes limitations such as features geometry or selectivity of the process depending on which mechanism is chosen [1].

In recent years, nano-ordered materials have attracted much attention since the products have been smaller in keeping with a trend of density growth or integration in various technology fields. They have great interest because of their potential to exhibit novel properties which cannot be achieved by bulk materials. For examples, two-(2D) and three-dimensionally (3D) ordered materials have attracted much interest due to their potential applications in photonic crystals [2–5], data storage [6–9], field emission device [10–13]. It is important to establish fabrication techniques of materials with desired shape or size depending on each application. For example, they must have periodic pillar or hole structures with high aspect ratio to use as 2D photonic crystals [11, 12]. It is necessary to be moth eye structure for use as antireflection coating [13, 14], which have pointed top preferably for field emission device [15].

Micromachining in a-silicon and silicon are widely employed for the fabrication of various micromechanical structures needed for many types of sensors and actuators Pattern transfer based on various etching processes plays an essential role in micromachining in the development of etching

processes for micromachining it is important to maintain high etch rate, good control of line width, good uniformity and high selectivity over both mask and underlying layer However, most of the traditional wet etchants are unable to meet these requirements for several reasons First, there is pure chemical reaction involved in the wet etching, resulting in an isotropic etching profile unless a crystal orientation dependent etch is used Secondly, adhesion of photoresist to the substrate is often poor due to the attack of the etchant Thirdly, surface tension of the liquid makes it impossible for the wet etchant to penetrate through very small windows in resist pattern and react with substrate Fourthly, gas bubble formation during the etching locally prevents the etching from proceeding and leads to poor uniformity Although some of the wet etchants for bulk micromachining, such as KOH or EDP, etch crystal silicon anisotropically, their etching characteristics strongly depend on the crystal orientation, doping concentration and electrical potential of the substrate As a result, the type, shape and size of the structures that can be realized are limited [16].

In previous reports, a variety of techniques for narrow nanogap fabrication have been demonstrated: electron beam lithography [17], [18], electromigration [19], mechanical break junction [20], sacrificial layer-assisted silicon and gold nanogaps [21], and surface-catalyzed chemical deposition [22]. However, except for electron beam lithography and sacrificial layer-assisted nanogaps, all other techniques have several problems in nanogap commercialization because of the complex steps and difficulties in fabricating reproducible nanogaps and their compatibility with other semiconductor circuits and processes. Therefore, new approaches and integration [23] methods for fabricating nanogap arrays need to be developed in order to overcome these problems.

On the other hand metallic nanoparticles have been used to establish self-assembly nanostructure of which physical and chemical properties have been investigated in recent years. In particular, gold nanoparticles can be easily prepared and have the characteristic of biocompatibility. Some new devices have been developed for the application of immunoassay by making use of the novel properties of nanostructure that is self-assembled by gold nanoparticles [24]. However, the properties of gold nanostructure can vary significantly with the size of gold nanoparticles and the pitch between gold nanoparticles in the nanostructures [24–26]. A gold-amplified sandwich immunoassay for the detection of human immunoglobulin G has also been developed by Natan and coworkers [26]. The sensitivity of their immunoassay can reach 1 pM. They have also conducted a series of studies on the effect of particle size and surface coverage on the detective sensitivity of immunoassay [27, 28].

A gap in a material with a high magnetic permeability causes magnetic field lines to leak into the surrounding ambient environment (air). If this gap is varied in size, the density of the field at a given point in that area will change. MEMS fabrication techniques enable the design and fabrication of a device that can take advantage of this behavior and locally modulate a static magnetic field [29].

2. METHODOLOGY

In this research, Si wafer is used to fabricate a micro and nanogap biosensor. The first step is to design and produce a mask, which is two mask designs are proposed, the amorphous silicon micro and nanogap with gold electrode process flow are develops. This research is mainly focus on the issue related to the fabrication of the micro and nanogap and the development of a new technology. The sidewall etching using IP-RIE to form thin micro and nanogap metal cantilevers which configured the 3-D micro and nanogap electrode grid array structure. Anisotropy of RIE is modeled and the etching profiles are simulated.

The starting material used in this research is a P-type, 100 mm in diameter (4 inch wafer) silicon-on-insulator (SOI) wafer as shown in Fig. 1.

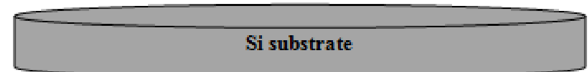

Figure 1: Si wafer

Silicon substrate (Si) wafer is used to reduce parasitic device capacitance and thus improve the final device performance.

The first process is to check the wafer type from its specification, measure wafer thickness (Si thickness), measure the sheet resistance. After that, lightly scribe the backside of each wafer; protect the top surface, using the scribe tool provided. Mark gently but make it visible and place scribed wafer in container.Wafer is cleaned before each process.

As for the lithography process, two photomasks are employed to fabricate the micro and nanogap using conventional photolithography and a-Si dry etching techniques. Commerical chrome mask is be used in

www.ijmer.com Vol.2, Issue.1, pp-009-015 ISSN: 2249-6645

this research for better photomasking process. This mask is used to develop the gold electrode with a-Si micro and nanogap pattern. The photomasks are designed using AutoCAD and then printed onto a chrome glass surface.

Fig. 2 is the first mask for micro and nanogap electrode formation which the length and width of 5000µm and 2500µm respectively.

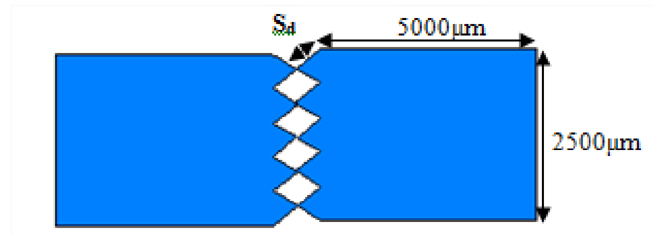

Figure 2: Design specification of the first Mask.

The proposed angle length of the end electrode are shown in Table 1. This is simply to check the best angle for the best micro and nanogap formation after etching process.

Table 1: Difference dimensions for S_d.

S_d	1	2	3	4	5	6
µm	*600*	*700*	*800*	*900*	*1000*	*1100*

The symbol S_d refer to the dimension for side angle of the design for micro and nanogap formation. Its show that when S_d is large this mean the micro and nanogap become very sharp and less sharp with less dimension of S_d.

Fig. 3 shows the actual arrangement of device design on chrome mask. It is consist of 160 dies with 6 different designs.

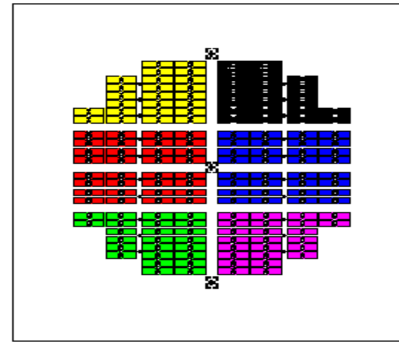

Figure 3: Schematic nanogap design of the actual mask1on chrome glass

Fig. 4 is a schematic device design of mask 2 with 5000μm length and 2500μm width. The distant between two rectangles is indicated as S_a bearing the same dimension with S_d according to the theory of Pythagoras, and the dimension of S_a can be defined mathematically as shown in figure 5.

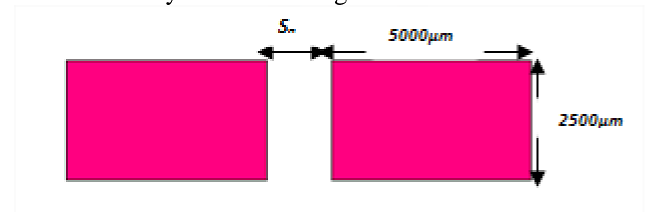

Figure 4: Design Specification for Mask2

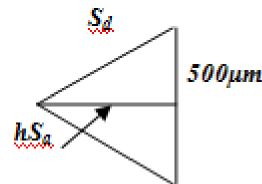

Figure 5: Schematic representation S_a, where $S_a=2hS_a$

Table 2: Variance Dimensions for S_a and S_d

S_d (µm)	600	700	800	900	1000	1100
$hS_a=((S_d)^2-(250)^2)^{1/2}$ (µm)	545	653	759	864	968	1071
$S_a=2\,hS_a$ (µm)	1090	1307	1516	1729	1963	2139

From the above table the dimension for S_a depend on the dimension of S_d. The calculated S_a is based on $S_a=2hS_a$

Fig. 6 is a schematic mask on chrome glass.

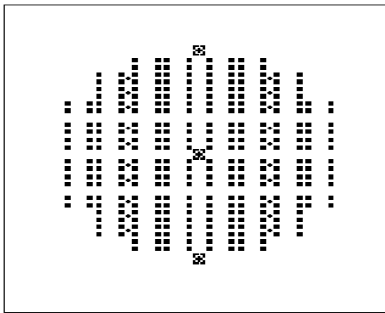

Figure 6: Schematic electrode Mask 2 on chrome glass

3. RESULTS AND DISCUSSIONS

The proposed process steps of gold electrode with a-Si micro and nanogap fabrication are shown in Figure 10. After cleaning the Si wafer, deposit 100nm silicon oxide layer over the Si wafer by using PECVD equipment then deposit 50nm a-Si layer on the silicon oxide surface using the same equipment PECVD before applied photolithography process, a layer of positive photoresist is first coating the a-Si surface, and then exposed to ultraviolet light through a mask 1. After development only the unexposed resist will remain. After that, applied dry etching process for a-Si pattern to fabricate the micro and nanogap for the micro and nanostructure using the recipe's parameters as explain in the Table 3.

Table3: RIE for a-Si recipe.

Cf_4	0
CHF_3	0
SF_6	50
O_2	10
Ar	30
Bais	250
Power ICP Power	650
APC/Control (Pa)	1.20
Etching Time	10 Sec

After remove the resist we can show by using SEM some damage in the photoresist layer for the pattern as shown in Fig. 7.

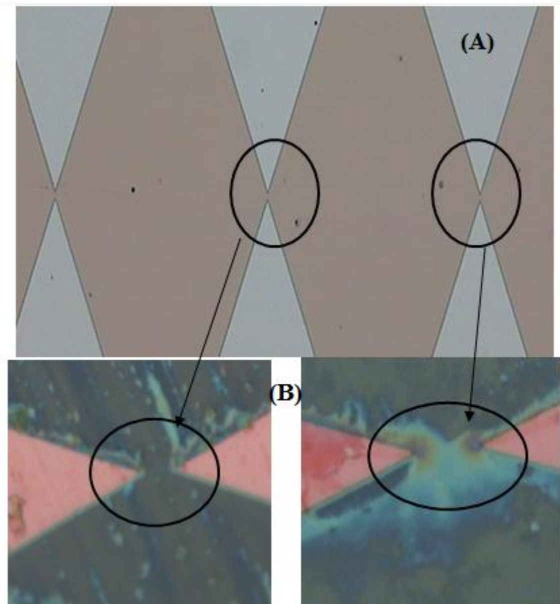

Figure 7: SEM photo for a-Si micro and nanogap:
A) Before using RIE process, B) after using RIE process.

It is clearly show that there is a problem in the gap and the size of the gap pattern, this affects negatively on the results of the examination for the electrical device characterization, and the proposed is depositing 135nm Al layer as a hard mask to avoid damage of the photoresist layer and the micro and nanogap structure during etching process by using the RIE. Next, in the photolithography process, a layer of positive photoresist is first applied on to the Al surface, and then exposed to ultraviolet light through a mask 1. After development only the unexposed resist will remain. After that a wet etching process of AL layer is performed using Al etch solution before removing the resist. After that, applied dry etching process for a-Si pattern by using same the recipe's parameters in the Table 3 to fabricate the micro and nanogap for the micro and nano structure, then applied wet etching to remove the Al layer, and Figure 8 show SEM image after applied dry RIE for the a-Si layer.

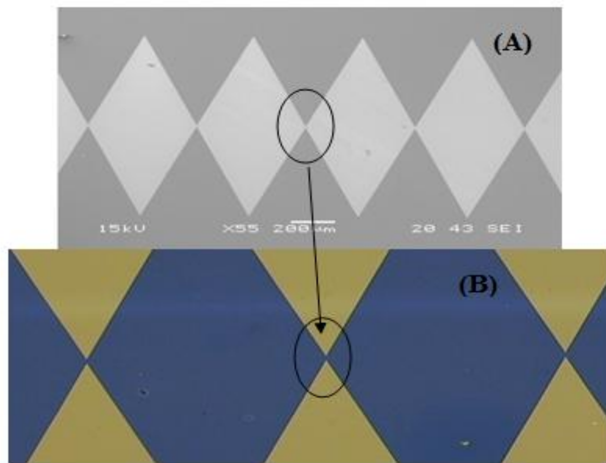

Figure 8: SEM image for a-Si micro and nangap pattern: (A) before using dry etching RIE, B) after using RIE.

It is clearly show that the change that took place in the amorphous silicon design after the deposition of the Al layer as a hard mask and how it has become sharper, and of course these positive results in the etching process lead to good results in the biodetection process because the RIE is an essential process in the micro and nano fabrication. Fig. 9 shows the planned the amount of fish and supply which was etching in the RIE process.

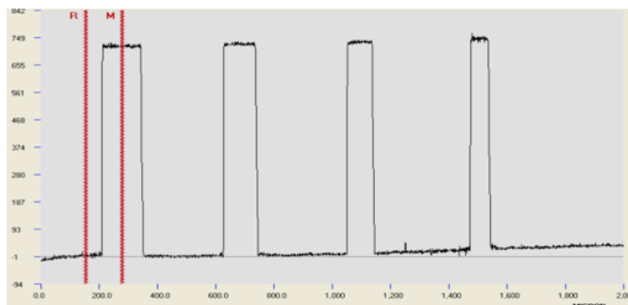

Figure 9: the thickness measurements for a-Si pattern after dry etching process.

The figure above it is clear that the RIE process applied to more than 70.0nm of the a-Si layer thickness and display the shape engraved up to 2000µm. After fabricate the gap, we proceed to fabricate the gold electrode where deposit a layer of 30nm/100nm for Ti/Au substrate as a first step to design the electrode, following the resist coating process. After exposing mask2 the layer of the resist is developed, then wet etching process of Ti/Au substrate is performed before removing the resist. Finally a structure of the gold electrode with a-Si micro and nanogap is obtained as in Fig. 10(h).

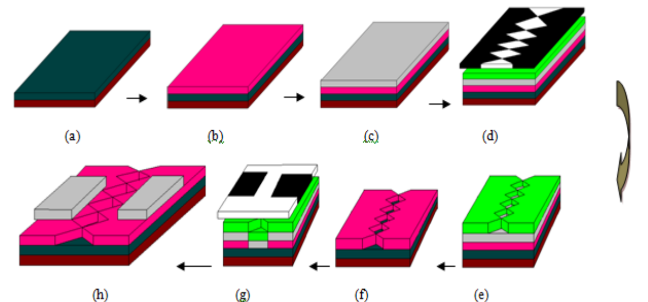

Figure 10: gold/ a-Silicon/ Silicon oxide structure process flow

An important issue in device fabrication is the ability to remove dry etch induced-damage in order to restore the electronic properties of the material. Really, the patterned Al was acted as a hard mask for protect the photoresist layer and a-Si pattern during the etching process. Laterally etch rate is obtained by measuring of image sizes difference between before and after etching with using SEM. In addition, the whole etching processes were done using IP reactive ion etching system with etching parameters of basic recipe as shown in Table 3 which then was further developed to control the nanostructure dimension.

Etch process needs a perfect result of just one step of nano patterns development, since stepped image development can lead to contaminations and then many porosities and un-etched areas result. On the other hand, resist patterns that were developed for sufficiently long time led to resist patterns that were removed of adjusted positions and they were even frequently solved in developer solution. However, optimum development time depends strongly on many parameters such as usage age of developer, resist thickness, soft bake time and density of patterns. In addition, higher patterns density led to longer development and etching times.

From the observation of experiment, the RIE mechanism is assumed to consist of both chemical and physical reaction in the chemical reaction, radicals as active gas molecules react with a-Si molecules and reacted formations are removed, consequently, the process becomes isotropic. Furthermore, this chemical reaction is activated by an impact of ions, that is, a kind of ion sputtering effect. This additive action is physical and has a directional characteristic owing to an incident angle of ions, usually perpendicular to the

electrodes (vertical). Under a certain etching condition, both the chemical and the physical reaction take place simultaneously, therefore, the etched shape may be decided by the ratio of each etch rate that can be defined as an instantaneous etch factor.

4. Conclusion

IPC-RIE has been developed successfully as a method to etch a-Si in a homogeneous way, independently of the grain orientation on the surface. A-Si micro and nanogap structure was produced and fabricated in this work. The etching rate measurements explain the stripping 1μm take 30sec for a-Si layer. These results are better than those using wet anisotropic etch techniques. The fabrication and development of micro and nanogap structure by using reactive ion etching (RIE) process need to deposit Al layer as a hard mask to avoid the damage during the etching.

5. ACKNOWLEDGMENT

We are grateful for fruitful discussions with our collaborators at the Institute of Nano Electronic Engineering (INEE) at University Malaysia Perlis (UniMAP). This work was supported by (INEE) at (UniMAP), through the Nano Technology project. The views expressed in this publication are those of the authors and do not necessarily reflect the official view of the funding agencies on the subject.

REFERENCES

[1] S. Winderbaum, O. Reinhold and F. Yun, Reactive ion etching (RIE) as a method for texturing polycrystalline silicon solar cells, *Solar Energy Materials and Solar Cells 46,* 1997, 239-248.

[2] E. Yablonovitch, Inhibited Spontaneous Emission in Solid-State Physics and Electronics, *Phys. Rev. Lett. 58,* 1987, 2059.

[3] V.V. Poborchii, Photonic-band-gap properties of two-dimensional lattices of Si nanopillars*, J. Appl. Phys. 91,* 2002, 3299.

[4] F. Pommereau, L. Legouezigou, G.H. Duan and B. Lombardet, Fabrication of low loss two-dimensional InP photonic crystals by inductively coupled plasma etching, *J. Appl. Phys. 95*, 2004, 2242.

[5] H.C. Guo, D. Nau, A. Ranke and H. Giessen., Large-area metallic photonic crystal fabrication with interference lithography and dry etching, *Appl. Phys. B. 81,* 2005, 271.

[6] I. Soten, H. Miguez, S.M. Yang, S. Petrov, N. Coombs, N. Tetreault, N. Matsuura, H.E. Ruda and G.A. Ozin, Barium Titanate Inverted Opals - Synthesis, Characterization, and Optical Properties, *Adv. Funct. Mater. 12,* 2002, 71.

[7]T. Aoki and M. Kuwabara, Micropatterned epitaxial (Pb,La)(Zr,Ti)O_3 thin films on Nb-doped $SrTiO_3$ substrates by a chemical solution deposition process with resist molds, *Appl. Phys. Lett. 27, 2004,* 2580.

[8]T. Aoki, M. Kondo, K. Kurihara, N. Kamehara and M. Kuwabara, Crystallinity of Microscopically Patterned (Pb,La)(Zr,Ti)O_3 Films on (001)Nb-Doped $SrTiO_3$ Substrates Prepared by Chemical Solution Deposition Process with Resist Molds, *J. Appl. Phys. 45,* 2006.

[9]J.E. Jang, S.N. Cha, Y. Choi, G.A.J. Ameratunga and D.J. Kang, Nanoscale capacitors based on metal-insulator-carbon nanotube-metal structures, *Appl. Phys. Lett. 87,* 2005, 263103.

[10]A.G. Rinzler, J.H. Hafner, P. Nikolaev, L. Lou and R.E. Smalley, Unraveling nanotubes: Field emission from an atomic wire, *Science 269,* 1995, 1550.

[11]V. Mizeikis, S. Juodkazis, J.Y. Ye, A. Rode, S. Matsuo and H. Misawa, Silicon surface processing techniques for micro-systems fabrication, *Thin Solid Films 438*, 2003, 445.

[12]V.V. Poborchii, A visible–near infrared range photonic crystal made up of Si nanopillars, *Appl. Phys. Lett. 75,* 1999, 3276.

[13]H. Toyota, K. Takahara, M. Okano, T. Yotsuya and H. Kikuta, Fabrication of Microcone Array for Antireflection Structured Surface Using Metal Dotted Pattern, *J. Appl. Phys. 40*, 2001, 747.

[14]D.H. Macdonald, A. Cuevas, M.J. Kerr, C. Samundsett and D. Ruby, Texturing industrial multicrystalline silicon solar cells, *Solar Energ.76,* 2004, 277.

[15]Minoru Mizuhata, Takuya Miyake, Yuki Nomoto and Shigehito Deki, Deep reactive ion etching (Deep-RIE) process for fabrication of ordered structural metal oxide thin films by the liquid phase infiltration method, *Microelectronic Engineering, 85,* 2008, 355–364.

[16]Y.X. Li, M.R. Wolffenbuttel, P.J French, M. Laros, P.M. Sarro and R.F. Wolffenbuttel, Reactive ion etching (RIE) techniques for micromachining applications, *Sensors and Actuators A, 41-42,* 1994, 317-323.

[17]P. B. Fischer and S. Y. Chou, 10 nm Electron Beam Lithography and Sub-50 nm Overlay Using a Modified Scanning Electron Microscope*, Appl. Phys. Lett., Vol. 62, No. 23,* 1993, 2989-2991.

[18]S. Itousa et al., Fabrication and AFM Characterization of a Coplanar Tunnel Junction with a Less Than 30 nm Interelectrode Gap, *Nanotechnology, vol. 5,* 1994, 19-25.

[19]H. Park et al., Fabrication of Metallic Electrodes with Nanometer Separation by Electromigration, *Appl. Phys. Lett., vol. 75, No. 2,* 1999, 301-303.

[20]M. A. Reed, Zhou C, Muller CJ, Conductance of a molecular junction, *Science, vol. 278 (5336),* 1997, 252-254.

[21]C.W. Park et al., Fabrication of Poly-Si/Au Nano-gaps Using Atomic-Layer-Deposited Al2O3 as a Sacrificial Layer, *Nanotechnology, 16*, 2005, 361-364.

[22]C.S. Ah et al., Fabrication of Integrated Nanogap Electrodes by Surface-Catalyzed Chemical Deposition, *Appl. Phys. Lett, 88,* 2006, 133116-1–113116-3.

[23]J. Kim et al., Integration of 5-V CMOS and High-Voltage Devices for Display Drive Applications, *ETRI Journal, vol. 20, 1*, 1998, 37-45.

[24]P.E. Buckle, R.J. Davies, T. Kinning, D. Yeung, P.R. Edwards, D. Pollard-Knight and C.R. Lowe. The resonant mirror: a novel optical sensor for direct sensing of biomolecular interactions part II: applications, *Biosens. Bioelectron. 8,* 1993, 355.

[25]K. Choi, H.J. Youn, Y.C. Ha, K.J. Kim and J.D. Choi, Detection of cholera cells using surface plasmon resonance sensor*, J. Microbiol. 36*, 1998, 43.

[26]L.A. Lyon, M.D. Musick and M.J. Natan, Colloidal Au-Enhanced Surface Plasmon Resonance Immunosensing, *Anal. Chem. 70*, 1998, 5177.

[27]L.A. Lyon, M.D. Musick, P.C. Smith, B.D. Reiss, D.J. Pena and M.J. Natan, Surface plasmon resonance of colloidal Au modified gold films, *Sensor. Actuator. B 54,* 1999, 118.

[28]L.A. Lyon, D.J. Pena and M.J. Natan, Surface Plasmon Resonance of Au Colloid-Modified Au Films: Particle Size Dependence, *J. Phys. Chem. B 103,* 1999, 5826.

[29]C.D. White, G. Piazza, P.J. Stephanou and A.P. Pisano, Design of nanogap piezoelectric resonators for mechanical RF magnetic field modulation, *Sensors and Actuators A 134,* 2007, 239–244.

ACKNOWLEDGEMENTS

An acknowledgement section may be presented after the conclusion, if desired.

REFERENCES

This heading is not assigned a number.

A reference list **MUST** be included using the following information as a guide. Only *cited* text references are included. Each reference is referred to in the text by a number enclosed in a square bracket (i.e., [3]). References **must be numbered and ordered according to where they are first mentioned in the paper,** NOT alphabetically.

Examples follow:

Journal Papers:

[1] M Ozaki, Y. Adachi, Y. Iwahori, and N. Ishii, Application of fuzzy theory to writer recognition of Chinese characters, *International Journal of Modelling and Simulation, 18(2),* 1998, 112-116.

Note that the journal title, volume number and issue number are set in italics.

Books:

[2] R.E. Moore, *Interval analysis* (Englewood Cliffs, NJ: Prentice-Hall, 1966).

Note that the title of the book is in lower case letters and italicized. There is no comma following the title. Place of publication and publisher are given.

Chapters in Books:

[3] P.O. Bishop, Neurophysiology of binocular vision, in J.Houseman (Ed.), *Handbook of physiology,* 4 (New York: Springer-Verlag, 1970) 342-366.

Note that the place of publication, publisher, and year of publication are enclosed in brackets. Editor of book is listed before book title.

Theses:

[4] D.S. Chan, *Theory and implementation of multidimensional discrete systems for signal processing*, doctoral diss., Massachusetts Institute of Technology, Cambridge, MA, 1978.

Note that thesis title is set in italics and the university that granted the degree is listed along with location information

Proceedings Papers:

[5] W.J. Book, Modelling design and control of flexible manipulator arms: A tutorial review, *Proc. 29th IEEE Conf. on Decision and Control*, San Francisco, CA, 1990, 500-506.

Note that the proceedings title is set in italic